Article

Guiding the High-Yield Synthesis of NHC-Ligated Gold Nanoclusters by ^{19}F NMR Spectroscopy

Hui Shen,[§] Xiongkai Tang,[§] Qingyuan Wu, Yuhao Zhang, Chuxin Ma, Zhen Xu, Boon K. Teo, and Nanfeng Zheng*

Cite This: ACS Nanosci. Au 2022, 2, 520−526 | Read Online

ACCESS | Metrics & More | Article Recommendations | Supporting Information

ABSTRACT: Optimizing the synthesis of atomically precise metal nanoclusters by virtue of molecular tools is highly desirable but quite challenging. Herein we report how ^{19}F NMR spectroscopy can be used to guide the high-yield synthesis of N-heterocyclic carbene (NHC)-stabilized gold nanoclusters. In spite of little difference, ^{19}F NMR signals of fluoro-incorporated NHCs (^{F}NHC) are highly sensitive to the tiny change in their surrounding chemical environments with different N-substituents, metals, or anions, thus providing a convenient strategy to discriminate species in reaction mixtures. By using ^{19}F NMR, we first disclosed that the one-pot reduction of ^{F}NHC-Au-X (X is halide) yields multiple compounds, including cluster compounds and also a large amount of highly stable $[Au(^{F}NHC)_2]^+$ byproduct. The detailed quantitative ^{19}F NMR analyses over the reductive synthesis of NHC-stabilized Au nanoclusters reveal that the formation of the di-NHC complex is deleterious to the high-yield synthesis of NHC-stabilized Au nanoclusters. With the understanding, the reaction kinetic was then slowed by controlling the reduction rate to achieve the high yield of a $[Au_{24}(^{F}NHC)_{14}X_2H_3]^{3+}$ nanocluster with a unique structure. The strategy demonstrated in this work is expected to provide an effective tool to guide the high-yield synthesis of organic ligand-stabilized metal nanoclusters.
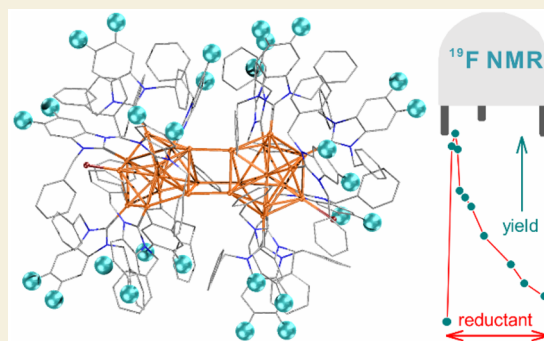
KEYWORDS: gold nanocluster, carbene ligand, kinetic control, high-yield synthesis, NMR spectroscopy

INTRODUCTION

Owing to their unique properties bridging single atoms and nanoparticles (NPs) as well as widespread applications in the fields of catalysis, biology, and electronics, atomically precise metal nanoclusters (NCs) have inspired great research passion.[1−5] Various synthetic methods have been developed in the past decades, giving rise to a rich library of coinage metal NCs with tailorable compositions, structures, and properties.[6−14] Nevertheless, the complexity of the reaction system, often involving multiple species within with different isomers present, has heavily prohibited the molecule-level understanding of their formation mechanism and thus the creation of a visible approach for the access to target NCs.[15] To probe the evolution process of cluster synthesis, some pioneers have employed mass spectrometry (MS) and ultraviolet−visible (UV−vis) spectroscopy to monitor the raw solution.[16] Remarkably, by using time-dependent electrospray ionization mass spectrometry (ESI-MS) and UV−vis spectroscopy, Xie's group was able to identify up to 29 intermediate species in the aging process of Au$_{25}$ superatoms.[17] A similar strategy has been employed to understand the transformation mechanisms of Au$_{25}$ to Au$_{44}$[18] and Au$_{23}$ to Au$_{25}$.[19]

Notwithstanding the significant progress, we envisage that more molecule characterization tools should be introduced to guide the synthesis of metal NCs, in the consideration that MS is usually limited to charged samples and UV−vis spectroscopy outputs just average information.[20,21] In this context, nuclear magnetic resonance (NMR) spectroscopy emerges an excellent candidate, which, when combined with MS and UV−vis, is able to comprehensively and accurately display all even intermediate species during their evolution process.[22] A close examination of the literature has revealed that ^{1}H and ^{31}P NMR spectroscopy have been widely employed in the community of metal NCs, including, but not limited to, structure deduction and purity confirmation of cluster compounds,[23] identification of practical precursors in the Brust-Schiffrin two-phase method,[24] characterization of hydride species in metal-hydride clusters,[25,26] as well as mechanism study of catalytic reactions.[27]
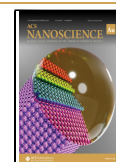
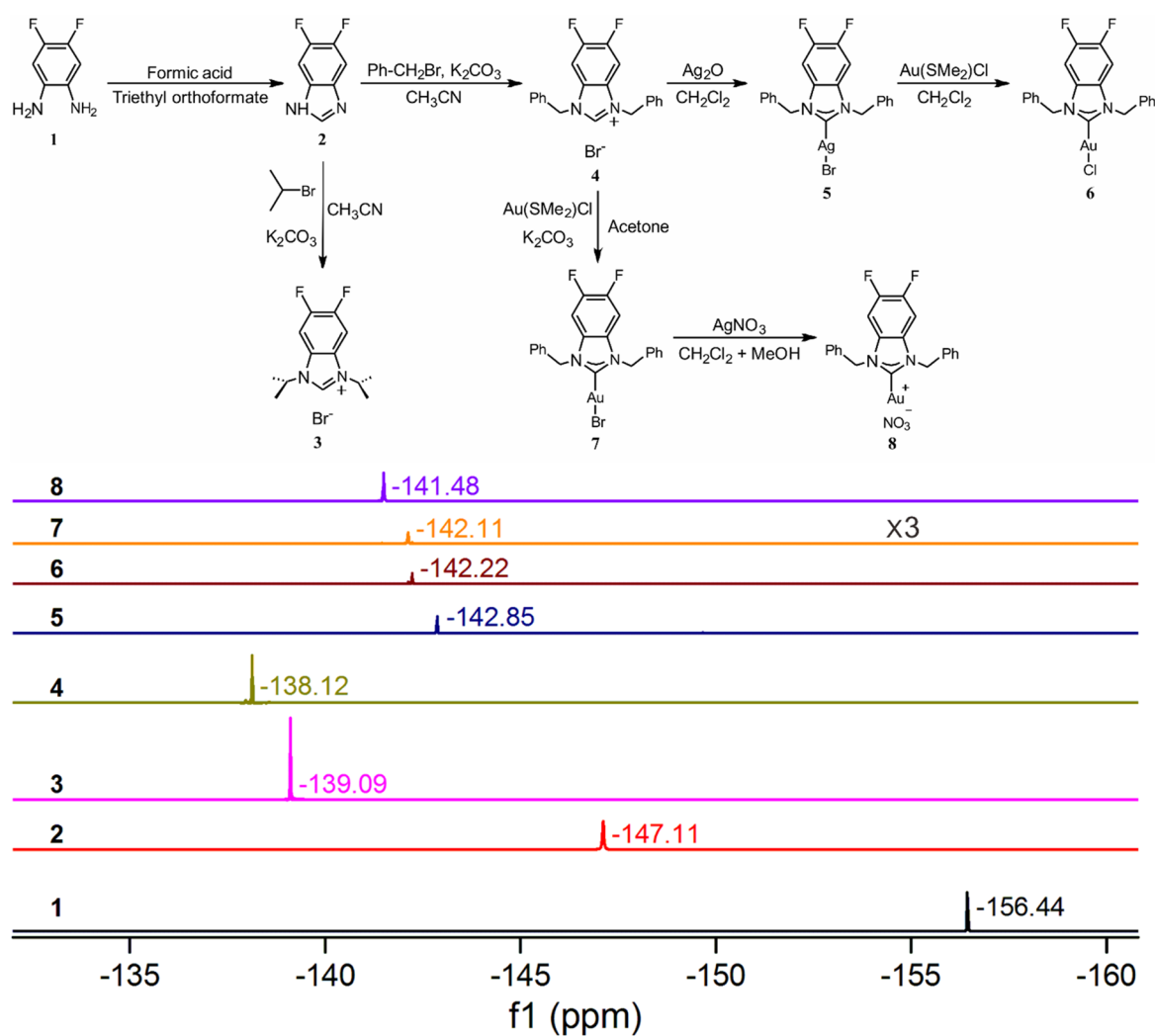In recent years, N-heterocyclic carbenes (NHCs) have been emerging as a new class of organic ligands for the stabilization

Figure 1. Synthesis and ^{19}F NMR spectra of F-labeled N-heterocyclic carbenes (^{F}NHC) and their different Ag and Au coordination compounds.

of coinage metal NCs, giving rise to a variety of metal NCs (e.g., Au$_3$, Au$_{11}$, Au$_{13}$, Au$_{25}$, Au$_{23}$, Au$_{44}$, Cu$_{31}$). The enhanced stability and promising applications in catalysis and biology of these metal NCs have been demonstrated.[28−38] Unfortunately, most of the reported NCs were synthesized in relatively low yields. To facilitate the study of new-born and promising materials, synthetic optimization is thus highly desirable. Of note, Crudden et al. fully tracked the formation and purification process of NHC-functionalized Au$_{11}$ and Au$_{13}$ NCs in previous studies by using ^{1}H, ^{31}P, and ^{13}C NMR spectroscopy, respectively.[28,31]

However, the application of NMR in monitoring reactions is limited by its low sensitivity and thus complexity. While ^{1}H NMR signals are easily overlapped, ^{13}C and ^{31}P ones offer limited sensitivity. Due to its high sensitivity, high resolution, broad chemical shift range, and capability to conduct quantitative analysis, ^{19}F NMR spectroscopy represents an excellent candidate for NC study.[39] Herein, we demontrate that ^{19}F NMR can serve as an effective tool in identifying "hidden" metal clusters in the reactions and thus helping to guide the cluster synthesis for the yield optimization. Although the methodology is generally applicable to different metal nanomaterial systems, the demonstration in this work focuses on the use of F-labeled NHC ligands stabilized Au NCs as an example.

RESULTS AND DISCUSSION

High Sensitivity of ^{19}F NMR to Remote Chemical Environment

The employment of ^{19}F NMR to monitor the synthesis process of metal NCs was initially inspired by the observation of distinct chemical shifts for different ^{F}NHC precursors (Figures S1−S8). As shown in Figure 1 and Figure S9, different structures result in distinct ^{19}F NMR, which is related to the electron accepting/donating nature of the substituents around a fluorine marker.[40,41] Among the listed compounds, the amino group of compound **1** features the strongest electron-donating ability, leading to the strongest shielding of electrons and the lowest chemical shift (−156.44 ppm). Similarly, the imidazole adjacent to the benzene ring in compound **2** is relatively electron-deficient, so its ^{19}F chemical shift moves to a lower field (−147.11 ppm). In sharp contrast to compounds **1** and **2**, the positively charged imidazole substituent of **3** and **4** is an extremely strong electron-withdrawing substituent, which endows them with high chemical shifts. The higher chemical shift of compound **4** (−138.12 ppm) than that of **3** (−139.09 ppm) can be rationalized by the higher electron-donating superconjugation effect of isopropyl than benzyl groups. With coordination to metal centers, compounds **5**, **6**, **7**, and **8** exhibit chemical shifts in the range of those between **2** and **3**. It

is reasonable that the imidazole ring acts as an electron donor after coordination to the metal atom, while the feedback effect of the metal atom in the NHC complex is rather weak. It is noteworthy that the weak coordination ability of nitrate in compound **8** leads to a partially positive charge of the Au atom, which suppresses the feedback effect of the metal atom even more and results in its high chemical shift. Totally, it occurs to us that ^{19}F NMR should be effective to distinguish different F-substituted compounds in the reaction mixture during the cluster synthesis.

On the basis of the above analysis, we employed ^{19}F NMR to track the raw products of NHC-stabilized Au NCs. A syringe pump was used to preciously control the addition speed of reductant (Figure S10). The preliminary synthesis was conducted by the chemical reduction of the $^{F}NHC-Au$-Br precursor in dichloromethane with excess $NaBH_4$ (1 equiv) in ethanol, in which an immediate color change from pale brown to dark brown was observed upon reduction (Figure 2a). After
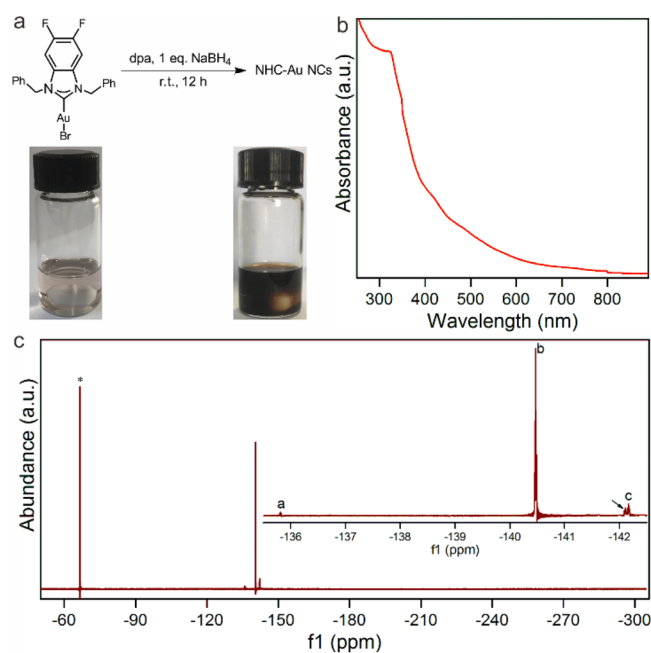

Figure 2. (a) Primary synthetic receipt of ^{F}NHC-protected gold NCs by reduction of $^{F}NHC-Au$-Br with 1 equiv amount of $NaBH_4$. (b) UV–vis spectroscopy of the corresponding raw product. (c) ^{19}F NMR of the raw product. Note: the peak marked as * is the internal standard of trifluorotoluene and that marked with arrow is $^{F}NHC-Au$-Br.

vigorously stirring for 12 h at room temperature, the UV–vis spectroscopy of the crude product showed weak peaks in the range 400–500 nm (Figure 2b), suggesting the formation of metal NCs. However, it was challenging to tell how many types of NCs were formed or whether other complexes were present from UV–vis results. As revealed by the ^{19}F NMR measurements (Figure 2c), at least three kinds of chemical shifts that were different from that of $^{F}NHC-Au$-Br precursor were observed in the raw product, among which one was dominant (peak b). A question naturally aroused is what the three compounds were.

Structure Characterization of Different Products in the Mixture

In order to collect enough crude products for the separation of each product, the reaction was scaled up. Column chromatography was used to separate the products (see the Supporting Information (SI) for the experimental details). After separation and purification, the three compounds, each of which displayed only single peak in ^{19}F NMR spectroscopy, were successfully attained (Figure 3a–c). To precisely determine their composition, we further used ESI-MS to characterize the compounds. The results revealed that one known NC, with the composition of $[Au_{25}(^{F}NHC)_{10}Br_2]^{2+}$ (peak a), was produced from the synthesis (Figure 3d and Figure S11a). To our surprise, the dominant peak (peak b) in the crude product belonged to $[Au(^{F}NHC)_2]^+$, a complex that was not highlighted in previous study (Figure 3e). The formula of the compound corresponding to peak c was assigned to $[Au_{24}(^{F}NHC)_{14}X_2H_3]^{3+}$ (hereafter abbreviated as $Au_{24}H_3$), a hydride-containing NHC-ligated Au NC (Figure 3f and Figure S11b–d).

We also characterized an individual component by using other techniques such as X-ray single-crystal diffraction (Figures S12–S20). Shown in Figure 3g is the total structure of $[Au_{25}(^{F}NHC)_{10}X_2]^{2+}$ cluster, whose core is composed of two icosahedra connected by sharing a vertex. Moreover, we have determined the structure of $[Au(^{F}NHC)_2]^+$ (peak "b"), in which the Au atom is linear coordinated by two ^{F}NHC ligands (Figure 3h). The presence of hydrides in $Au_{24}H_3$ cluster has been verified by measuring the ESI-MS of the product synthesized from $NaBD_4$, in which the peak is shifted ~1 Da as a comparison (Figure 3i).

X-ray crystallographic analysis uncovers the structure of the novel cluster. A closely related cluster has been synthesized by an independent method with a yield of 16–18% during the preparation of this paper.[42] As shown in Figure 4a, the $Au_{24}H_3$ cluster is composed of a Au_{24} core, 14 ^{F}NHC ligands, and two halides. The Au_{24} core (Figure 4b) can be anatomized as the connection of two Au_{12} units through triangular faces, constructing a trigonal prismatic. The Au_{12} motif is derived from centered icosahedron, with interestingly the lack of an apex. Within the Au_{12} unit, Au–Au lengths between central Au and surrounding ones are in the range 2.705–2.781 Å while those between the surrounding ones were 2.771–3.006 Å. The Au–Au bond distances between the two Au_{12} give an average value of 2.706 Å. We note that the joining style of the core is highly different from that of $[Au_{24}(PPh_3)_{10}(SC_2H_4Ph)_5Cl_2]^+$, where the two identical Au_{12} motifs are linked together through pentagon faces.[43] The binding motifs and free electrons of the $Au_{24}H_3$ cluster, however, are in parallel with DFT optimized $[Au_{22}(dppe)_3(PPh_3)_8H_3]^{3+}$ (dppe is 1,2-bis(diphenylphosphino)ethane and PPh_3 is triphenylphosphine).[44] Both clusters feature 16 free electrons, 3 hydrides, and 6 bridging Au atoms. The 14 ^{F}NHC ligands of $Au_{24}H_3$ cluster coordinate to the metal moiety tightly, with average Au–C bond lengths of 2.053 Å. The bromides bind with top Au atoms with an average bond length of 2.415 Å. Interestingly, in the cluster, six uncoordinated Au sites are observed, indicating the efficiency of bulky NHCs in the creation of surface uncoordinated active sites.[35,45] Although the structure of $[Au_{24}(^{F}NHC)_{14}X_2H_3]^{3+}$ in this work is almost the same as that of $[Au_{24}(NHC)_{14}Cl_2H_3]^{3+}$ reported very recently,[42] the stability of $[Au_{24}(^{F}NHC)_{14}X_2H_3]^{3+}$ was much more stable than $[Au_{24}(NHC)_{14}Cl_2H_3]^{3+}$ without fluoro-
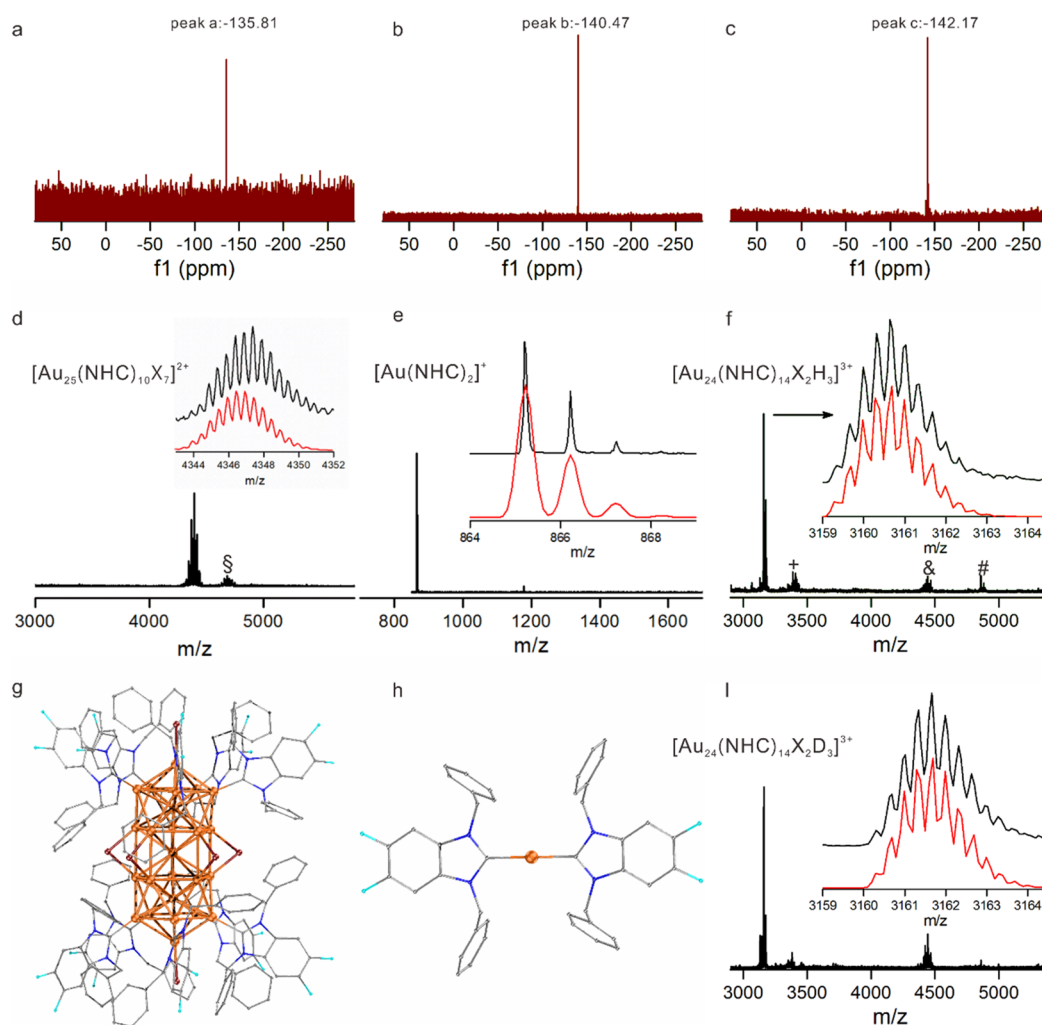
Figure 3. Characterization of individual product separated from the raw product. (a−c) ^{19}F NMR and (d−f) ESI-MS spectroscopy of the product of peaks "a", "b", and "c", respectively. Note: the § peak in (d) corresponds to $[Au_{25}(^FNHC)_{10}X_2+^FNHC\text{-}Au\text{-}X]^{2+}$. The peaks of +, &, and # in (f) correspond to $[Au_{24}(^FNHC)_{14}X_2H_3+^FNHC\text{-}Au\text{-}X]^{3+}$, $[Au_{24}(^FNHC)_{14}X_2H_3\text{-}^FNHC\text{-}Au^+]^{2+}$, and $[Au_{24}(^FNHC)_{14}X_2H_3(SbF_6)]^{2+}$, respectively. (g and h) Structures of $[Au_{25}(^FNHC)_{10}Br_2]^{2+}$ (peak "a") and $[Au(^FNHC)_2]^+$ (peak "b"). (i) ESI-MS of the product of peak "c" synthesized from NaBD$_4$, showing the presence of three hydrides in the cluster. For (d−f) and (i), the insets are the comparison of experimental (black trace) and simulated (red trace) isotopic patterns.

groups on NHC ligands. While $[Au_{24}(^FNHC)_{14}X_2H_3]^{3+}$ was stable upon thermal treatment at 65 °C in air, $[Au_{24}(NHC)_{14}Cl_2H_3]^{3+}$ was demonstrated to convert to Au$_{13}$ upon heating at 45 °C. This result clearly indicates that the substituents in the backbone of NHCs play an important role in determining the stability of NHC-stabilized metal NCs.

The Au$_{24}$H$_3$ cluster exhibits molecule-like UV−vis spectrum in dichloromethane, with distinct peaks at 300, 520, and 690 nm, respectively (Figure 4c). To our surprise, the cluster, although involving active hydrides on structure, displays high stability.[46] As shown in Figure 4d, the cluster in the solution form can survive for at least 12 h upon heating at 65 °C in air, again illustrating the great power of NHCs in the stabilization of metal NCs.[28,31,33−36,38] Of particular interest to us from the stability evaluation of title and reported Au$_{24}$H$_3$ clusters is that the two clusters exhibit distinct thermal stability. It suggests that the ligand structure, involving substituents in the backbone of NHCs as revealed herein, plays an important role in determining stability.[28,47] The new structure, hydride-incorporation, and presence of uncoordinated metal sites as

well as high stability of the cluster suggest its potential application in the field of catalysis and hydrogen storage.[44]

^{19}F NMR Helps Optimize the Synthesis of Au$_{24}$H$_3$ Clusters

The forgoing discussion shows how the ^{19}F NMR spectroscopy is an effective strategy to distinguish an individual component in cluster mixtures, and in the following section, we thereby set out to optimize the synthesis of the target product of Au$_{24}$H$_3$ NCs by employing time-resolved ^{19}F NMR to track the synthesis. Benefitted from the quantitative analysis of the ^{19}F NMR peaks, the yield of each component in the raw solution during the evolution process can be precisely determined. As shown in Figure 5a, the original $^FNHC-Au-Br$ ^{19}F-NMR signal decreases dramatically upon reduction within 1 h, yielding mainly the $[Au(^FNHC)_2]^+$ byproduct, along with small quantities of the sought-after metal clusters (10% yield based on ^FNHC ligands). It is noteworthy that the yield of the byproduct $[Au(^FNHC)_2]^+$ in the initial synthetic prototype can be up to 80%, indicating its robustness toward reduction. In fact, we also find that $[Au(^FNHC)_2]^+$ is resistant to reduction by NaBH$_4$ (Figure S21). These results suggest that the

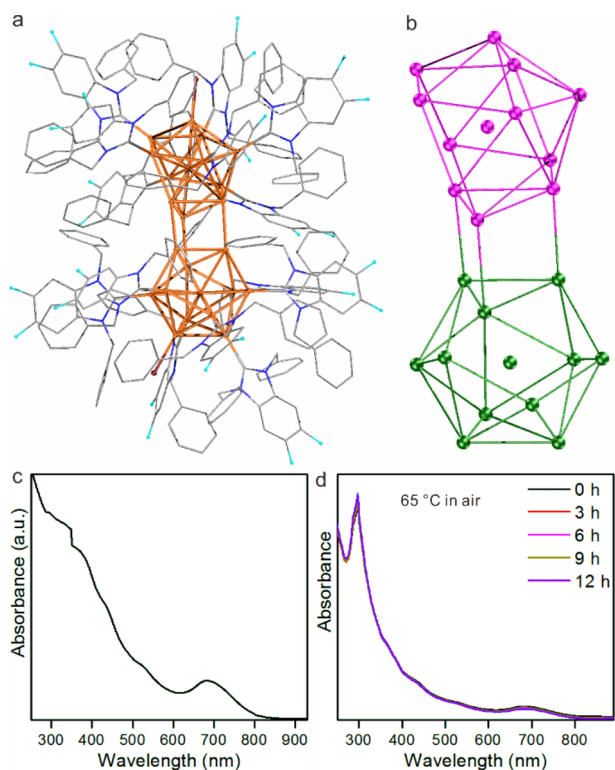**Figure 4.** Characterization of the NHC-stabilized gold-hydride NCs. (a and b) Total and core structure of $[Au_{24}(^FNHC)_{14}X_2H_3]^{3+}$ cluster. Color legend: orange, magenta, and green, Au; red, Br; turquoise, F; blue, N; gray, C. All hydrogen atoms are omitted for clarity. (c) UV–vis spectrum of $Au_{24}H_3$ cluster in dichloromethane. (d) Stability test of $Au_{24}H_3$ cluster in 1,2-dichloroethane at 65 °C.
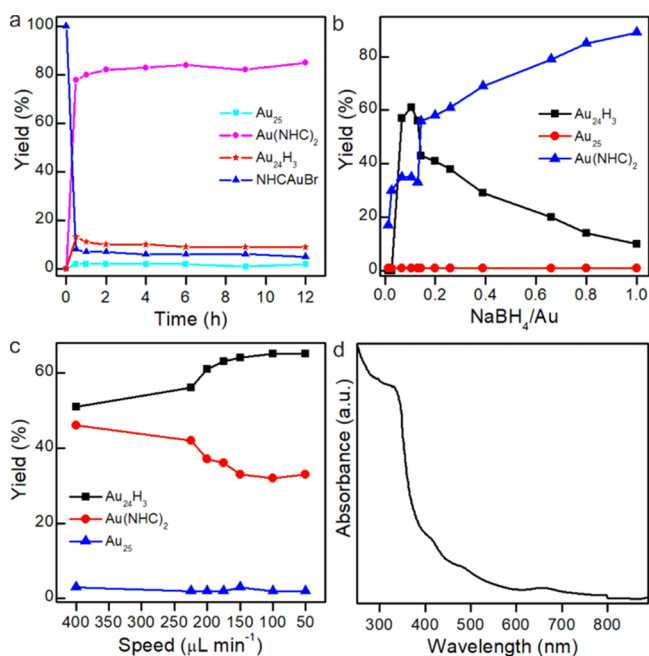

Figure 5. (a) Time-dependent yield of each product in the raw solution using the primary synthetic receipt. Note: total yield of all products in the solution has been normalized in the calculation. (b) Yield of each product in terms of amount of $NaBH_4$. (c) Effect of addition speed of reductant on yield of each product. Note: The point of 400 μL min^{-1} was estimated with $NaBH_4$ added in one portion. (d) UV–vis spectroscopy of raw product in the optimal conditions.

formation of highly stable di-NHC complex is the main reason for the low yield of the NCs.

In the following section, we then attempt to slow down the reduction kinetics, thereof inhibiting the production of $[Au(^FNHC)_2]^+$ byproduct and enhancing the yield of the metal clusters. In this context, two approaches have been devised, namely, (1) controlling the reductant/metal ratio and (2) slowing down the speed of adding the reductant. The results are as follows. (1) As expected, by tailoring the stoichiometry of $NaBH_4$ in the synthesis, we are able to obtain a maximum yield of 61% at the optimal $NaBH_4$/Au of 1:10, a much high value in comparison to the initial synthesis. The ratio below this value cannot reduce the precursor efficiently, while those above it give rise to an excess (undesired) amount of $[Au(^FNHC)_2]^+$ (Figure 5b). (2) Reducing the speed of the addition of $NaBH_4$ enhances the yield of the metal clusters (Figure 5c) further. The optimal yield can be raised by nearly 6-fold to 63%. It is interestingly observable that the raw solution before and after optimization exhibits distinct colors (Figure S22), and the one in the optimal conditions displays distinguished characteristics of $Au_{24}H_3$ NCs (Figure 5d).

CONCLUSION

In conclusion, ^{19}F NMR spectroscopy has been demonstrated as an effective tool in studying the synthesis process of ligand stabilized metal nanoclusters. Due to its sensitivity toward chemical environment and quantitative analysis, we have succeeded in tracking the reaction process of a novel gold-hydride nanocluster stabilized by F-labeled NHCs and preciously pointed out the main factor in influencing its yield. Moreover, the yield of target nanoclusters has been optimized with the aid of ^{19}F NMR. Overall, the work presents a molecule-level strategy for parallel exploration of structural diversity and chemical purity of metal nanostructures, which may facilitate the study on surface coordination chemistry of metal nanomaterials.

ASSOCIATED CONTENT

Supporting Information

The Supporting Information is available free of charge at https://pubs.acs.org/doi/10.1021/acsnanoscienceau.2c00026.

> Discussions of experiemental details, figures of ^1H NMR spectra for all compounds, ^{19}F NMR spectra, syringe pump photo, experimental and simulated isotopic patterns, photographs of single crystals, ORTEP diagrams, packing structures, and photographs of different reactions, and tables of crystal data and structure refinement (PDF)

Accession Codes

CCDC 2126309, 2159531, and 2159533 contain the supplementary crystallographic data for this paper. 2117208 contain the supplementary crystallographic data for this paper. These data can be obtained free of charge via www.ccdc.cam.ac.uk/data_request/cif, or by emailing data_request@ccdc.cam.ac.uk, or by contacting The Cambridge Crystallographic Data Centre, 12 Union Road, Cambridge CB2 1EZ, UK; fax: + 44 1223 336033

AUTHOR INFORMATION

Corresponding Author

Nanfeng Zheng − *State Key Laboratory for Physical Chemistry of Solid Surfaces, Collaborative Innovation Center of Chemistry for Energy Materials, and National & Local Joint Engineering Research Center for Preparation Technology of Nanomaterials, College of Chemistry and Chemical Engineering, Xiamen University, Xiamen 361005, China; Innovation Laboratory for Sciences and Technologies of Energy Materials of Fujian Province (IKKEM), Xiamen 361005, China;* orcid.org/0000-0001-9879-4790; Email: nfzheng@xmu.edu.cn

Authors

Hui Shen − *State Key Laboratory for Physical Chemistry of Solid Surfaces, Collaborative Innovation Center of Chemistry for Energy Materials, and National & Local Joint Engineering Research Center for Preparation Technology of Nanomaterials, College of Chemistry and Chemical Engineering, Xiamen University, Xiamen 361005, China*

Xiongkai Tang − *State Key Laboratory for Physical Chemistry of Solid Surfaces, Collaborative Innovation Center of Chemistry for Energy Materials, and National & Local Joint Engineering Research Center for Preparation Technology of Nanomaterials, College of Chemistry and Chemical Engineering, Xiamen University, Xiamen 361005, China*

Qingyuan Wu − *State Key Laboratory for Physical Chemistry of Solid Surfaces, Collaborative Innovation Center of Chemistry for Energy Materials, and National & Local Joint Engineering Research Center for Preparation Technology of Nanomaterials, College of Chemistry and Chemical Engineering, Xiamen University, Xiamen 361005, China*

Yuhao Zhang − *State Key Laboratory for Physical Chemistry of Solid Surfaces, Collaborative Innovation Center of Chemistry for Energy Materials, and National & Local Joint Engineering Research Center for Preparation Technology of Nanomaterials, College of Chemistry and Chemical Engineering, Xiamen University, Xiamen 361005, China;* orcid.org/0000-0002-2014-4373

Chuxin Ma − *State Key Laboratory for Physical Chemistry of Solid Surfaces, Collaborative Innovation Center of Chemistry for Energy Materials, and National & Local Joint Engineering Research Center for Preparation Technology of Nanomaterials, College of Chemistry and Chemical Engineering, Xiamen University, Xiamen 361005, China*

Zhen Xu − *State Key Laboratory for Physical Chemistry of Solid Surfaces, Collaborative Innovation Center of Chemistry for Energy Materials, and National & Local Joint Engineering Research Center for Preparation Technology of Nanomaterials, College of Chemistry and Chemical Engineering, Xiamen University, Xiamen 361005, China*

Boon K. Teo − *State Key Laboratory for Physical Chemistry of Solid Surfaces, Collaborative Innovation Center of Chemistry for Energy Materials, and National & Local Joint Engineering Research Center for Preparation Technology of Nanomaterials, College of Chemistry and Chemical Engineering, Xiamen University, Xiamen 361005, China*

Complete contact information is available at:
https://pubs.acs.org/10.1021/acsnanoscienceau.2c00026

Author Contributions

§H.S. and X.T. contributed equally. CRediT: **Hui Shen** conceptualization (equal), data curation (equal), formal analysis (equal), investigation (equal), methodology (lead), project administration (equal), validation (equal), visualization (lead), writing-original draft (equal), writing-review & editing (equal); **Xiongkai Tang** data curation (equal), formal analysis (equal), investigation (lead), methodology (equal); **Qingyuan Wu** data curation (supporting), formal analysis (supporting), investigation (supporting), writing-review & editing (supporting); **Yuhao Zhang** investigation (supporting); **Chuxin Ma** investigation (supporting); **Zhen Xu** investigation (supporting); **Boon K. Teo** project administration (supporting); **Nanfeng Zheng** conceptualization (equal), formal analysis (equal), funding acquisition (lead), resources (lead), supervision (lead), writing-original draft (equal).

Notes

The authors declare no competing financial interest.

REFERENCES

(1) Jadzinsky, P. D.; Calero, G.; Ackerson, C. J.; Bushnell, D. A.; Kornberg, R. D. Structure of a Thiol Monolayer-Protected Gold Nanoparticle at 1.1 Å Resolution. *Science* **2007**, *318*, 430−433.

(2) Takano, S.; Tsukuda, T. Chemically Modified Gold/Silver Superatoms as Artificial Elements at Nanoscale: Design Principles and Synthesis Challenges. *J. Am. Chem. Soc.* **2021**, *143*, 1683−1698.

(3) Du, Y. X.; Sheng, H. T.; Astruc, D.; Zhu, M. Z. Atomically Precise Noble Metal Nanoclusters as Efficient Catalysts: A Bridge between Structure and Properties. *Chem. Rev.* **2020**, *120*, 526−622.

(4) Shen, H.; Tian, G.; Xu, Z.; Wang, L.; Wu, Q.; Zhang, Y.; Teo, B. K.; Zheng, N. F. N-heterocyclic carbene coordinated metal nanoparticles and nanoclusters. *Coord. Chem. Rev.* **2022**, *458*, 214425.

(5) Jin, R. C.; Zeng, C. J.; Zhou, M.; Chen, Y. X. Atomically Precise Colloidal Metal Nanoclusters and Nanoparticles: Fundamentals and Opportunities. *Chem. Rev.* **2016**, *116*, 10346−10413.

(6) Yao, Q. F.; Chen, T. K.; Yuan, X.; Xie, J. P. Toward Total Synthesis of Thiolate-Protected Metal Nanoclusters. *Acc. Chem. Res.* **2018**, *51*, 1338−1348.

(7) Sharma, S.; Chakrahari, K. K.; Saillard, J. Y.; Liu, C. W. Structurally Precise Dichalcogenolate-Protected Copper and Silver Superatomic Nanoclusters and Their Alloys. *Acc. Chem. Res.* **2018**, *51*, 2475−2483.

(8) Tang, Q.; Hu, G. X.; Fung, V.; Jiang, D. E. Insights into Interfaces, Stability, Electronic Properties, and Catalytic Activities of Atomically Precise Metal Nanoclusters from First Principles. *Acc. Chem. Res.* **2018**, *51*, 2793−2802.

(9) Takano, S.; Hasegawa, S.; Suyama, M.; Tsukuda, T. Hydride Doping of Chemically Modified Gold-Based Superatoms. *Acc. Chem. Res.* **2018**, *51*, 3074−3083.

(10) Ghosh, A.; Mohammed, O. F.; Bakr, O. M. Atomic-Level Doping of Metal Clusters. *Acc. Chem. Res.* **2018**, *51*, 3094−3103.

(11) Konishi, K.; Iwasaki, M.; Shichibu, Y. Phosphine-Ligated Gold Clusters with Core plus exo Geometries: Unique Properties and Interactions at the Ligand-Cluster Interface. *Acc. Chem. Res.* **2018**, *51*, 3125−3133.

(12) Hossain, S.; Niihori, Y.; Nair, L. V.; Kumar, B.; Kurashige, W.; Negishi, Y. Alloy Clusters: Precise Synthesis and Mixing Effects. *Acc. Chem. Res.* **2018**, *51*, 3114−3124.

(13) Aikens, C. M. Electronic and Geometric Structure, Optical Properties, and Excited State Behavior in Atomically Precise Thiolate-

Stabilized Noble Metal Nanoclusters. *Acc. Chem. Res.* **2018**, *51*, 3065−3073.

(14) Shen, H.; Xu, Z.; Wang, L.; Han, Y.; Liu, X.; Malola, S.; Teo, B. K.; Häkkinen, H.; Zheng, N. F. Tertiary Chiral Nanostructures from C−H···F Directed Assembly of Chiroptical Superatoms. *Angew. Chem., Int. Ed.* **2021**, *60*, 22411−22416.

(15) Goswami, N.; Yao, Q. F.; Chen, T. K.; Xie, J. P. Mechanistic exploration and controlled synthesis of precise thiolate-gold nanoclusters. *Coord. Chem. Rev.* **2016**, *329*, 1−15.

(16) Qian, H.; Jin, R. C. Controlling Nanoparticles with Atomic Precision: The Case of $Au_{144}(SCH_2CH_2Ph)_{60}$. *Nano Lett.* **2009**, *9*, 4083−4087.

(17) Luo, Z.; Nachammai, V.; Zhang, B.; Yan, N.; Leong, D. T.; Jiang, D. E.; Xie, J. P. Toward Understanding the Growth Mechanism: Tracing All Stable Intermediate Species from Reduction of Au(I)−Thiolate Complexes to Evolution of Au_{25} Nanoclusters. *J. Am. Chem. Soc.* **2014**, *136*, 10577−10580.

(18) Yao, Q. F.; Yuan, X.; Fung, V.; Yu, Y.; Leong, D. T.; Jiang, D. E.; Xie, J. P. Understanding seed-mediated growth of gold nanoclusters at molecular level. *Nat. Commun.* **2017**, *8*, 927.

(19) Yao, Q. F.; Fung, V.; Sun, C.; Huang, S.; Chen, T. K.; Jiang, D. E.; Lee, J.; Xie, J. P. Revealing isoelectronic size conversion dynamics of metal nanoclusters by a noncrystallization approach. *Nat. Commun.* **2018**, *9*, 1979.

(20) Chen, T. K.; Yao, Q. F.; Nasaruddin, R. R.; Xie, J. P. Electrospray Ionization Mass Spectrometry: A Powerful Platform for Noble-Metal Nanocluster Analysis. *Angew. Chem., Int. Ed.* **2019**, *58*, 11967−11977.

(21) Chakraborty, I.; Pradeep, T. Atomically Precise Clusters of Noble Metals: Emerging Link between Atoms and Nanoparticles. *Chem. Rev.* **2017**, *117*, 8208−8271.

(22) Agrachev, M.; Ruzzi, M.; Venzo, A.; Maran, F. Nuclear and Electron Magnetic Resonance Spectroscopies of Atomically Precise Gold Nanoclusters. *Acc. Chem. Res.* **2019**, *52*, 44−52.

(23) Xiao, K.; Zhao, Y.; Zhu, J.; Zhao, L. Hyperconjugative aromaticity and protodeauration reactivity of polyaurated indoliums. *Nat. Commun.* **2019**, *10*, 5639.

(24) Goulet, P. J. G.; Lennox, R. B. New Insights into Brust-Schiffrin Metal Nanoparticle Synthesis. *J. Am. Chem. Soc.* **2010**, *132*, 9582−9584.

(25) Sun, C. F.; Mammen, N.; Kaappa, S.; Yuan, P.; Deng, G.; Zhao, C.; Yan, J. Z.; Malola, S.; Honkala, K.; Häkkinen, H.; Teo, B. K.; Zheng, N. F. Atomically Precise, Thiolated Copper−Hydride Nanoclusters as Single-Site Hydrogenation Catalysts for Ketones in Mild Conditions. *ACS Nano* **2019**, *13*, 5975−5986.

(26) Yuan, X.; Sun, C.; Li, X. H.; Malola, S.; Teo, B. K.; Häkkinen, H.; Zheng, L.; Zheng, N. F. Combinatorial Identification of Hydrides in a Ligated Ag_{40} Nanocluster with Noncompact Metal Core. *J. Am. Chem. Soc.* **2019**, *141*, 11905−11911.

(27) Fu, F.; Xiang, J.; Cheng, H.; Cheng, L.; Chong, H.; Wang, S. X.; Li, P.; Wei, S.; Zhu, M. Z.; Li, Y. A Robust and Efficient Pd_3 Cluster Catalyst for the Suzuki Reaction and Its Odd Mechanism. *ACS Catal.* **2017**, *7*, 1860−1867.

(28) Narouz, M. R.; Osten, K. M.; Unsworth, P. J.; Man, R. W. Y.; Salorinne, K.; Takano, S.; Tomihara, R.; Kaappa, S.; Malola, S.; Dinh, C. T.; Padmos, J. D.; Ayoo, K.; Garrett, P. J.; Nambo, M.; Horton, J. H.; Sargent, E. H.; Häkkinen, H.; Tsukuda, T.; Crudden, C. M. N-heterocyclic carbene-functionalized magic-number gold nanoclusters. *Nat. Chem.* **2019**, *11*, 419−425.

(29) Robilotto, T. J.; Bacsa, J.; Gray, T. G.; Sadighi, J. P. Synthesis of a Trigold Monocation: An Isolobal Analogue of $[H_3]^+$. *Angew. Chem., Int. Ed.* **2012**, *51*, 12077−12080.

(30) Jin, L.; Weinberger, D. S.; Melaimi, M.; Moore, C. E.; Rheingold, A. L.; Bertrand, G. Trinuclear Gold Clusters Supported by Cyclic (alkyl)(amino)carbene Ligands: Mimics for Gold Heterogeneous Catalysts. *Angew. Chem., Int. Ed.* **2014**, *53*, 9059−9063.

(31) Narouz, M. R.; Takano, S.; Lummis, P. A.; Levchenko, T. I.; Nazemi, A.; Kaappa, S.; Malola, S.; Yousefalizadeh, G.; Calhoun, L. A.; Stamplecoskie, K. G.; Häkkinen, H.; Tsukuda, T.; Crudden, C. M.

Robust, Highly Luminescent Au_{13} Superatoms Protected by N-Heterocyclic Carbenes. *J. Am. Chem. Soc.* **2019**, *141*, 14997−15002.

(32) Yi, H.; Osten, K. M.; Levchenko, T. I.; Veinot, A. J.; Aramaki, Y.; Ooi, T.; Nambo, M.; Crudden, C. M. Synthesis and enantioseparation of chiral Au_{13} nanoclusters protected by bis-N-heterocyclic carbene ligands. *Chem. Sci.* **2021**, *12*, 10436−10440.

(33) Shen, H.; Xiang, S. J.; Xu, Z.; Liu, C.; Li, X. H.; Sun, C. F.; Lin, S. C.; Teo, B. K.; Zheng, N. F. Superatomic Au_{13} clusters ligated by different N-heterocyclic carbenes and their ligand-dependent catalysis, photoluminescence, and proton sensitivity. *Nano Res.* **2020**, *13*, 1908−1911.

(34) Shen, H.; Deng, G.; Kaappa, S.; Tan, T.; Han, Y.; Malola, S.; Lin, S. C.; Teo, B. K.; Häkkinen, H.; Zheng, N. F. Highly Robust but Surface-Active: An N-Heterocyclic Carbene-Stabilized Au_{25} Nanocluster. *Angew. Chem., Int. Ed.* **2019**, *58*, 17731−17735.

(35) Shen, H.; Xu, Z.; Hazer, M.; Wu, Q.; Peng, J.; Qin, R.; Malola, S.; Teo, B. K.; Häkkinen, H.; Zheng, N. F. Surface Coordination of Multiple Ligands Endows N-Heterocyclic Carbene-Stabilized Gold Nanoclusters with High Robustness and Surface Reactivity. *Angew. Chem., Int. Ed.* **2021**, *60*, 3752−3758.

(36) Peltier, J. L.; Soleilhavoup, M.; Martin, D.; Jazzar, R.; Bertrand, G. Absolute Templating of M(111) Cluster Surrogates by Galvanic Exchange. *J. Am. Chem. Soc.* **2020**, *142*, 16479−16485.

(37) Hirano, K.; Takano, S.; Tsukuda, T. Ligand Effects on the Structures of $[Au_{23}L_6(C{\equiv}CPh)_9]^{2+}$ (L = N-Heterocyclic Carbene vs Phosphine) with Au_{17} Superatomic Cores. *J. Phys. Chem. C* **2021**, *125*, 9930−9936.

(38) Shen, H.; Wang, L.; López-Estrada, O.; Hu, C.; Wu, Q.; Cao, D.; Malola, S.; Teo, B. K.; Häkkinen, H.; Zheng, N. F. Copper-hydride nanoclusters with enhanced stability by N-heterocyclic carbenes. *Nano Res.* **2021**, *14*, 3303−3308.

(39) Jackson, J. C.; Hammill, J. T.; Mehl, R. A. Site-Specific Incorporation of a ^{19}F-Amino Acid into Proteins as an NMR Probe for Characterizing Protein Structure and Reactivity. *J. Am. Chem. Soc.* **2007**, *129*, 1160−1166.

(40) Saunders, C.; Khaled, M. B.; Weaver, J. D.; Tantillo, D. J. Prediction of ^{19}F NMR Chemical Shifts for Fluorinated Aromatic Compounds. *J. Org. Chem.* **2018**, *83*, 3220−3225.

(41) Pike, S. J.; De Poli, M.; Zawodny, W.; Raftery, J.; Webb, S. J.; Clayden, J. Diastereotopic fluorine substituents as ^{19}F NMR probes of screw-sense preference in helical foldamers. *Org. Biomol. Chem.* **2013**, *11*, 3168−3176.

(42) Kulkarni, V. K.; Khiarak, B. N.; Takano, S.; Malola, S.; Albright, E. L.; Levchenko, T. I.; Aloisio, M. D.; Dinh, C. T.; Tsukuda, T.; Häkkinen, H.; Crudden, C. M. N-Heterocyclic Carbene-Stabilized Hydrido Au_{24} Nanoclusters: Synthesis, Structure, and Electrocatalytic Reduction of CO_2. *J. Am. Chem. Soc.* **2022**, *144*, 9000−9006.

(43) Das, A.; Li, T.; Nobusada, K.; Zeng, Q.; Rosi, N. L.; Jin, R. C. Total Structure and Optical Properties of a Phosphine/Thiolate-Protected Au_{24} Nanocluster. *J. Am. Chem. Soc.* **2012**, *134*, 20286−20289.

(44) Gao, Z.; Wei, K.; Wu, T.; Dong, J.; Jiang, D. E.; Sun, S.; Wang, L. A Heteroleptic Gold Hydride Nanocluster for Efficient and Selective Electrocatalytic Reduction of CO_2 to CO. *J. Am. Chem. Soc.* **2022**, *144*, 5258−5262.

(45) Gou, X.; Liu, T.; Wang, Y.; Han, Y. Ultrastable and Highly Catalytically Active N-Heterocyclic-Carbene-Stabilized Gold Nanoparticles in Confined Spaces. *Angew. Chem., Int. Ed.* **2020**, *59*, 16683−16689.

(46) Takano, S.; Hirai, H.; Muramatsu, S.; Tsukuda, T. Hydride-Doped Gold Superatom $(Au_9H)^{2+}$: Synthesis, Structure, and Transformation. *J. Am. Chem. Soc.* **2018**, *140*, 8380−8383.

(47) Zhang, X.; Yang, H.; Zhao, X.; Wang, Y.; Zheng, N. F. The effects of surface ligands and counter cations on the stability of anionic thiolated $M_{12}Ag_{32}$ (M = Au, Ag) nanoclusters. *Chin. Chem. Lett.* **2014**, *25*, 839−843.